

# IMAGE STABILIZATION BASED ON FUSING THE VISUAL INFORMATION IN DIFFERENTLY EXPOSED IMAGES

*Marius Tico, Markku Vehvilainen*

Nokia Research Center  
P.O.Box 100, FI-33721 Tampere, Finland  
Email: tico@ieee.org

## ABSTRACT

The objective of image stabilization is to prevent or remove the motion blur degradation from images. We introduce a new approach to image stabilization based on combining information available in two differently exposed images of the same scene. In addition to the image normally captured by the system, with an exposure time determined by the illumination conditions, a very shortly exposed image is also acquired. The difference between the exposure times of the two images determines differences in their degradations which are exploited in order to recover the original image of the scene. We formulate the problem as a maximum a posteriori (MAP) estimation based on the degradation models of the two observed images, as well as by imposing an edge-preserving image prior. The proposed method is demonstrated through a series of simulation experiments, and visual examples on natural images.

**Index Terms**— image stabilization, motion blur, image restoration, exposure time, image deconvolution

## 1. INTRODUCTION

The problem addressed by image stabilization dates since the beginning of photography, and it is basically caused by the fact that any known image sensor needs to have the image projected on it during a period of time called integration (exposure) time. Any motion of the camera during this time causes a shift of the image projected on the sensor resulting in a degradation of the final image, called motion blur. This image degradation dramatically influences the user perception of the imaging product performance, and hence the manufacturers prioritize their efforts for developing robust and efficient solutions to this problem. The main driven factors motivating this work include:

- The need for longer integration times in order to cope with smaller pixel areas that result from sensor miniaturization and resolution increase requirements. Thus, the smaller the pixel area the less photons/second could be captured by the pixel and hence a longer integration time is needed for good results.
- The need for longer integration times in order to acquire better pictures in low light conditions.
- The difficulty to avoid unwanted motion during the integration time when using high zoom, and/or small hand-held devices.

Various methods for removing or preventing the motion blur degradation have been proposed. The existent solutions can be divided in two categories based on whether they are aiming to correct or to prevent the motion blur degradation. In the first category

are those solutions that are aiming for restoring a motion blurred image shot captured during a longer exposure time. If the point spread function (PSF) of the motion blur is known then the original image could be restored, up to some level of accuracy, by applying an image deconvolution approach [1]. However, in practice the motion blur PSF is unknown, since its structure is determined by the arbitrary camera motion during the exposure time. The lack of knowledge about the blur PSF suggests the use of blind deconvolution approaches in order to restore the motion blurred images [2, 3]. Unfortunately, most of these methods rely on rather simple motion models, e.g. linear constant speed motion, and hence their potential use in consumer products is rather limited. One way to estimate the motion blur PSF is based on measurements of the camera motion during the exposure time. Such an approach have been introduced in [4], where the authors proposed the use of an extra camera in order to acquire motion information during the exposure time of the principal camera.

In order to cope with the unknown motion blur process, designers have adopted solutions able to prevent such blur for happening in the first place. In this category are included all optical image stabilization (OIS) solutions adopted nowadays by many camera manufactures. These solutions are utilizing inertial sensors (gyroscopes) in order to measure the camera motion, following then to cancel the effect of this motion by moving either the image sensor, or some optical element in the opposite direction. Apart of cost and size disadvantages associated with these solutions, their are less effective for longer exposure times when the mechanism may drift, producing motion blurred images. A different method, based on specially designed CMOS sensors has been proposed in [5]. The method utilizes the possibility to independently control the exposure time of each image pixel, following to prevent motion blur by interrupting the integration time of those pixels where motion is detected.

In a previous work [6], we introduced an approach to image stabilization based on fusing multiple short exposed image frames of the same scene. Due to their short exposure the individual image frames are less affected by motion blur and more affected by noise. The camera motion, that would otherwise blur a long exposed image, determines misalignment between the captured image frames, and hence its effect can be canceled by registering and fusing the image frames. Due to various limitations in computational resources a smaller number of image frames might be preferable in some systems. In this paper we address such a solution where the number of frames used for image stabilization is reduced to two. One of the image frames is captured with a normal exposure time in the given illumination conditions, and the second image is captured with a very short exposure time. Due to differences in their exposure times the two images will be degraded differently. Thus, the underexposed

image is mainly affected by noise, whereas the normal-exposed image might be affected by motion blur. In our previous work [7], we presented an approach to motion blur PSF (point spread function) identification based on two differently exposed image frames. The estimated PSF was then used to recover the original image by applying a ML (maximum likelihood) de-convolution algorithm [1]. In this paper we present a further development of our previous work, aiming for improving the sensitivity to errors in motion blur PSF estimation, by designing a combined MAP (maximum a posteriori) estimation of both latent image and motion blur PSF.

## 2. THE PROPOSED METHOD

Let us denote the two observed images of the scene by  $g_1$  and  $g_2$  respectively. In the following we assume that the two images are registered one with respect to another such that at any pixel coordinate  $\mathbf{x} = (x, y)$ , the values  $g_1(\mathbf{x})$  and  $g_2(\mathbf{x})$  denote different representations of the same physical area of the scene. It is to be noted here that, the registration of the two images must be able to cope with their different degradations, and hence a registration algorithm robust to such image degradation is needed. In our work we used the algorithm proposed in [8].

The degradation models of the two observed images driven by their different exposure times, are formulated as follows. The normal exposed image ( $g_1$ ) is a representation of the original image  $f$ , that might be affected by motion blur, as well as a zero mean additive noise:

$$g_1(\mathbf{x}) = d(\mathbf{x}) * f(\mathbf{x}) + n_1(\mathbf{x}), \quad (1)$$

where  $d$  denotes the motion blur PSF (point spread function),  $n_1$  denotes the additive zero mean noise term, and  $*$  stands for two-dimensional convolution operator.

The additional, short exposed image  $g_2$ , is a noisy representation of the original image that is assumed to be unaffected by motion blur

$$\alpha e(\mathbf{x}) * g_2(\mathbf{x}) = f(\mathbf{x}) + n_2(\mathbf{x}), \quad (2)$$

where  $\alpha$  is a luminance scale factor that accounts for the lower brightness of  $g_2$  due to shorter exposure,  $e(\mathbf{x})$  is a point spread function that, in accordance to the assumed model is the Dirac delta function ( $\delta(\mathbf{x})$ ), and  $n_2$  denotes an additive noise. The additional point spread function  $e(\mathbf{x})$  was introduced here in order to model the residual blurring between  $g_2$  and intermediate estimates of the latent image  $f$ . For tractability, both noise terms  $n_1$  and  $n_2$  are assume zero mean Gaussian with variances  $\sigma_1^2$  and  $\sigma_2^2$ . Also, we note that the two noise terms should have very different powers due to different exposure times of the two observed images, i.e.  $\sigma_1^2 \ll \sigma_2^2$ .

The joint posterior probability density function (p.d.f.) of the original image  $f$  and blur PSFs  $d$  and  $e$  is given by

$$p(f, d, e | g_1, g_2) \sim p(g_1 | f, d) p(g_2 | f, e) p(f) p(d, e), \quad (3)$$

from where retaining only the terms which depend of  $f$ ,  $d$  or  $e$  we obtain the MAP objective function

$$Q(f, d, e) = -\log p(g_1 | f, d) - \log p(g_2 | f, e) - \log p(f) - \log p(d, e). \quad (4)$$

The first two terms of (4) can be derived from the observation models formulated in (1) and (2):

$$\begin{aligned} -\log p(g_1 | f, d) &\sim \lambda_1 / 2 \sum_{\mathbf{x} \in \Omega} [g_1(\mathbf{x}) - f(\mathbf{x}) * d(\mathbf{x})]^2, \\ -\log p(g_2 | f, e) &\sim \lambda_2 / 2 \sum_{\mathbf{x} \in \Omega} [\alpha e(\mathbf{x}) * g_2(\mathbf{x}) - f(\mathbf{x})]^2, \end{aligned} \quad (5)$$

where  $\lambda_i = \sigma_i^{-2}$ ,  $i = 1, 2$ , and  $\Omega$  denotes the 2D image domain.

In order to avoid over-smoothing the image, we adopt a discrete form of the Total Variation (TV) prior for the latent image

$$-\log p(f) \sim \gamma \sum_{\mathbf{x} \in \Omega} |\nabla f(\mathbf{x})| \quad (6)$$

where  $\nabla$  stands for spatial gradient operator, and  $\gamma$  is the prior weight which balances our confidence between the prior and the observations. In our work we assumed a Gamma distribution for the prior weight  $\gamma$ , i.e.  $\gamma \sim \Gamma(\gamma | a, b)$ , following to re-estimate the parameter at each iteration step based on the current estimate of the latent image.

The model that we used for the two PSFs was selected such that to be optimized when  $e$  becomes identical to Dirac delta function. This is:

$$\begin{aligned} -\log p(d, e) &\sim \beta_1 / 2 \sum_{\mathbf{x} \in \Omega} [d(\mathbf{x}) * e(\mathbf{x}) - d(\mathbf{x})]^2 \\ &+ \beta_2 / 2 \sum_{\mathbf{x} \in \Omega} [e(\mathbf{x}) - \delta(\mathbf{x})]^2, \end{aligned} \quad (7)$$

where  $\beta_1$  and  $\beta_2$  are positive values weighting the importance of the PSF prior.

Joining (5), (6) and (7) we obtain the final form of the objective function, whose optimization is achieved as shown in the following algorithm.

---

### Algorithm 1

*Input:* Registered images  $g_1, g_2$ , and a rough estimate of the size of PSF support.

*Output:* The latent image  $f$

*Initialization:*  $k = 0$ ,  $f^{(k)} = g_2$ ,  $\epsilon_k = \infty$

*Iteration:*

1. Minimize with fix  $f$ :  $\hat{d}, \hat{e} \leftarrow \operatorname{argmin}_{d, e} Q(f^{(k)}, d, e)$
  2. Update PSF:  $d^{(k)}(\mathbf{x}) = \hat{d}(\mathbf{x}) * \hat{e}(\mathbf{x})$
  3. Enhance  $d^{(k)}$  by removing noise and normalization
  4. Minimize with fix  $d$ :  $f^{(k+1)} \leftarrow \operatorname{argmin}_f Q(f, d^{(k)}, \delta)$ , by iterating from initial guess  $f = g_1$
  5. Calculate  $\epsilon_{k+1} = \|d * f^{(k+1)} - g_1\|$
  6. If  $\epsilon_{k+1} > \epsilon_k$ , then stop iteration and return  $f = f^{(k)}$
- 

In the first step of the algorithm the objective function is minimized with respect to  $d$  and  $e$ . This can be achieved by solving the system of equations obtained when equating with zero the gradients of  $Q$  with respect to  $d$  and  $e$ . For efficiency we implemented this step in the Fourier domain.

The second step of the algorithm can be also performed in the Fourier domain following then to recover the spatial domain representation of the blur PSF by inverse Fourier transform, based also on the PSF support size estimate provided to the algorithm.

The third step of the algorithm aims for enhancing the spatial representation ( $d^{(k)}$ ) of the blur PSF, by canceling its noisy coefficients. In order to distinguish the noisy coefficients from the real PSF coefficients we analyze the 2D PSF signal  $d^{(k)}$  at different levels of smoothness, obtained by iterative low pass filtering. A threshold is established at each level based on the standard deviation at that level, and all coefficient that are below the threshold are canceled. Finally,

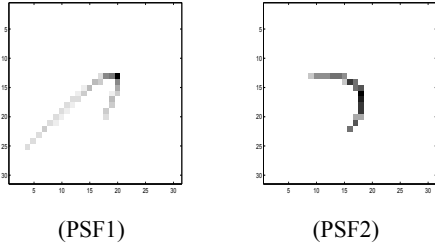


**Fig. 1.** Simulated PSFs used in the experiments.

we cancel in  $d^{(k)}$  all coefficients that have been canceled at any one of the levels considered. The remaining non-zero coefficients of  $d^{(k)}$  are then normalized such that to some up to unity, in accordance to the energy conservation assumption, i.e.  $\sum d(\mathbf{x}) = 1$ .

The fourth step of the proposed algorithm consists of minimizing the objective function with respect to  $f$ , for the given PSF. The gradient of the objective function with respect to  $f$  is given by

$$\begin{aligned} \nabla_f Q &= \lambda_1 [f(\mathbf{x}) * d^{(k)}(\mathbf{x}) - g_1(\mathbf{x})] * d^{(k)}(-\mathbf{x}) \\ &+ \lambda_2 [f(\mathbf{x}) - \alpha g_2(\mathbf{x})] + \gamma \nabla [w(\mathbf{x}) \nabla f(\mathbf{x})], \end{aligned} \quad (8)$$

where  $w(\mathbf{x}) = 1/|\nabla f(\mathbf{x})|$  is the diffusive coefficient. In our work we minimize the objective function with respect to  $f$  by applying the conjugate gradient (CG) iteration and lagging the diffusive coefficient one iteration behind. Convergence is relatively fast due to CG properties, and we stop the CG iterations when the relative change in the objective function between two consecutive iterations is smaller than a given threshold. It is important to emphasize also that the prior parameter  $\gamma$  is updated in each iteration based on the latent image estimated so far. Thus at iteration  $i$  we have

$$\gamma_i = \frac{a - 1}{b + (1/N) \sum_{\mathbf{x} \in \Omega} |\nabla f_i(\mathbf{x})|}, \quad (9)$$

where  $N$  denotes the number of pixels in the image, and  $a, b$  are the parameters of the Gamma distribution imposed for the weight  $\gamma$ .

### 3. EXPERIMENTS

The proposed algorithm has been evaluated through a series of experiments including numerical simulations as well as visual inspections on natural images. The values of the algorithmic parameters used in our experiments are selected as follows. The parameter  $\alpha$  is estimated as the ratio between the average luminance of the two input images. The parameters of the prior Gamma distribution have been fixed to  $a = 4$  and  $b = 1$ . The parameters for PSF priors are  $\beta_1 = \beta_2 = 1$ . The PSF support was assumed of size  $31 \times 31$  in all experiments.

In our simulation experiments we used "Lenna" and "Camera-man" images corrupted by various levels of noise, and different blur PSFs in order to simulate differently exposed image pairs. The motion blur PSFs used in these simulations are shown in Fig. 1. The blurs have nonlinear trajectories and they correspond to motions of different velocities. Thus, some portions of PSF1 are less prominent corresponding to fast motion moments, whereas PSF2 is more emphasized corresponding to a slow motion speed.

The short exposed image in each simulation was created by adding zero mean Gaussian noise to the original image using "imnoise" rou-

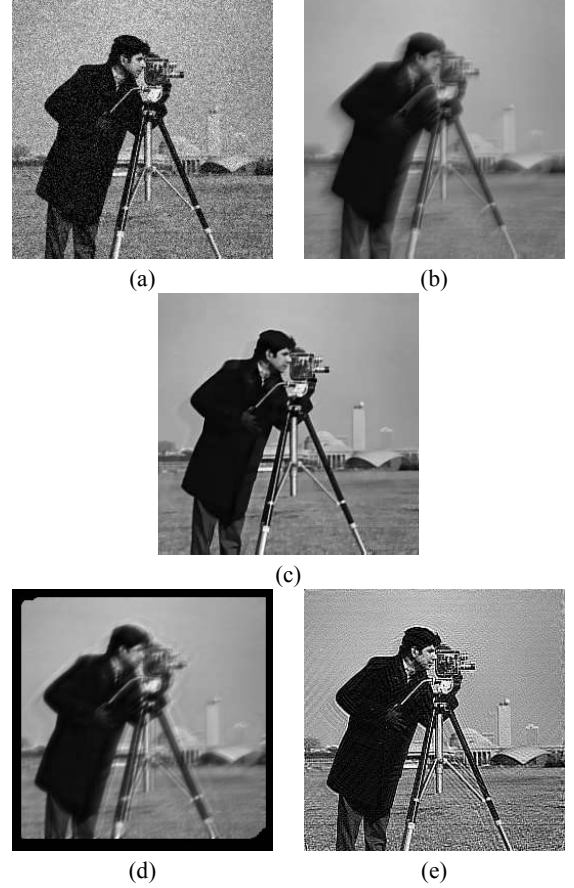


**Fig. 2.** Visual comparison: (a,b) the simulated short and long exposed images corrupted by noise (STD 0.1), and blur (PSF1) respectively, (c) the result of the proposed algorithm, (d) Matlab "deconvblind", and (e) ML deconvolution.

tine of Matlab, and the normal exposed image was simulated by convolving the original image with a certain blur PSF.

Table 1 summarizes the results obtained in several simulations on both images. A number of 10 simulations have been done for each line in the table by using different realizations of the additive noise which affects the short exposed image. The average and standard deviation of the PSNRs (Peak Signal to Noise Ratios) of the restored images are shown in the table. The improvement in the PSNR, denoted IPSNR in the table, was calculated between the restored image and the highest PSNR input image. We note that the algorithm is able to achieve an improvement of several decibels even for relatively large levels of noise present in the short exposed image. Moreover, due to the use of TV image prior the result is more robust to errors in PSF estimation, canceling most of the artifacts commonly generated by an ML de-convolution algorithm, as shown in Fig. 2 (e). The figure shows also a visual comparison between the result achieved by the proposed algorithm (Fig. 2 (c)), and the result achieved by using the routine "deconvblind" of Matlab (Fig. 2 (d)). For this test we provided to all methods the first estimate of the blur PSF produced by our algorithm, and we selected the best result, in the PSNR sense, provided by the Matlab routine in 200 iterations.

Two visual examples on real images captured with a digital cam-

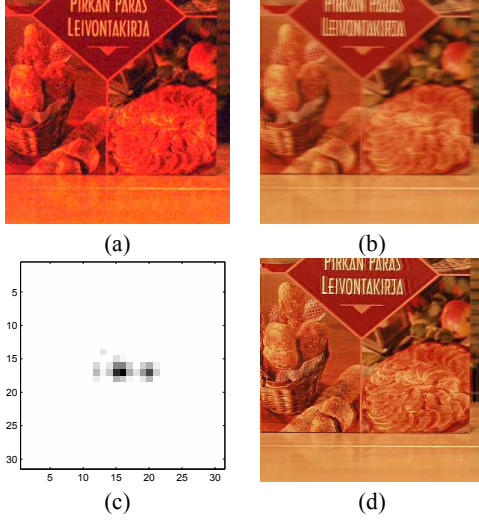


**Fig. 3.** Real image example: (a,b) the short and normal exposed images respectively, (c) the estimated PSF, (d) the restored image.

Blur PSF	Noise STD (normalized)	PSNR (dB) avg (std)	IPSNR (dB)
Cameraman			
PSF1	0.1	26.4 (0.7)	5.8
PSF1	0.2	25.4 (1.5)	6.3
PSF2	0.1	27.7 (1.0)	7.1
PSF2	0.2	26.8 (0.7)	7.3
Lenna			
PSF1	0.1	31.3 (0.2)	5.3
PSF1	0.2	29.5 (0.1)	7.1
PSF2	0.1	31.5 (1.4)	5.5
PSF2	0.2	29.3 (0.8)	6.2

**Table 1.** The results of simulation experiments.

era are shown in Fig. 3, and Fig. 4. In both cases the shutter speed of the camera for the short and normal exposed images have been set at 1/100 sec, and 1 sec respectively.

#### 4. CONCLUSIONS

We presented a method for image restoration from motion blur degradation based on the availability of two differently exposed image shots of the same scene. The method relies on MAP estimation of the latent image of the scene by exploiting the differences in the degradation models of the two input images. The proposed algorithm has been demonstrated through a series of experiments including numerical simulations and visual examples on real images.

#### 5. REFERENCES

[1] P.A. Jansson, *Deconvolution of image and spectra*, Academic Press, 1997.  
 [2] Tony F. Chan and Chiu-Kwong Wong, “Total Variation Blind Deconvolution,” *IEEE Transactions on Image Processing*, vol. 7, no. 3, pp. 370–375, 1998.



**Fig. 4.** Low light image example, from up to bottom we have the short exposed, the normal exposed, and the restored image.

[3] Yu-Li You and M. Kaveh, “A regularization approach to joint blur identification and image restoration,” *IEEE Trans. on Image Processing*, vol. 5, no. 3, pp. 416–428, Mar. 1996.  
 [4] Moshe Ben-Ezra and Shree K. Nayar, “Motion-Based Motion Deblurring,” *IEEE Transactions on Pattern Analysis and Machine Intelligence*, vol. 26, no. 6, pp. 689–698, 2004.  
 [5] Xinqiao Liu and Abbas El Gamal, “Synthesis of high dynamic range motion blur free image from multiple captures,” *IEEE Transaction on Circuits and Systems-I*, vol. 50, no. 4, pp. 530–539, 2003.  
 [6] Marius Tico and Markku Vehvilainen, “Robust image fusion for image stabilization,” in *IEEE International Conference on Acoustics, Speech, and Signal Processing (ICASSP)*, Honolulu, USA, 2007.  
 [7] Marius Tico, Mejdi Trimeche, and Markku Vehvilainen, “Motion blur identification based on differently exposed images,” in *Proc. of the IEEE International Conference of Image Processing (ICIP)*, Atlanta, GA, USA, Oct. 2006, pp. 2021–2024.  
 [8] Marius Tico, Sakari Alenius, and Markku Vehvilainen, “Method of motion estimation for image stabilization,” in *IEEE International Conference on Acoustics, Speech, and Signal Processing (ICASSP)*, Toulouse, France, 2006, vol. 2, pp. 277–280.